Food Control 143 (2023) 109290

Contents lists available at ScienceDirect

Food Control

journal homepage: www.elsevier.com/locate/foodcont

Texture profile and short-NIR spectral vibrations relationship evaluated through Comdim: The case study for animal and vegetable proteins

Marcela de Souza Zangirolami [a], Thaysa Fernandes Moya Moreira [b], Fernanda Vitória Leimann [a,c], Patrícia Valderrama [a], Paulo Henrique Março [a,*]

[a] Post-Graduation Program of Food Technology, Federal University of Technology of the Paraná State (UTFPR), CEP 87301-899, Campo Mourão, Paraná, Brazil
[b] Post-Graduation Program of Food Science, State University of Maringá (UEM), CEP 87020-900, Maringá, Paraná, Brazil
[c] Centro de Investigação de Montanha (CIMO), Instituto Politécnico de Bragança, Campus de Santa Apolónia, 5300-253, Bragança, Portugal

ARTICLE INFO

Keywords:
Protein sources
ComDim
PCA
Near-infrared
Chemometrics

ABSTRACT

Important parameters related to the acceptance of a food can be investigated by the texture profile analysis (TPA), which has as a drawback the time and sample-consuming characteristic. In this sense, the development of a method to integrate the texture parameters into a fast and non-destructive analysis, such as the near-infrared (NIR) spectroscopy, can contribute to better quality control for food products. In this sense, this study aimed to compare commercial samples of proteins from animal and plant sources to find the relation between NIR vibrations and TPA parameters through principal component analysis (PCA) and multiblock data analysis of common dimensions (ComDim). To do so, it was necessary to use a strategy to measure the TPA of powder proteins, which was done by producing a ¼ (m:m) flour: protein dough. The results indicated that animal proteins are related to adhesiveness and springiness and correlated to the NIR region from 1120 to 1180 nm and 1300–1460 nm. The plant proteins are characterized by their high cohesiveness, chewiness, gumminess, hardness, and resilience correlated to the NIR regions between 900 and 1120 nm, 1180–1220 nm, 1250–1295 nm, and 1460–1700 nm.

1. Introduction

The consumption of protein derived from animal sources is a common human practice due to its high biological value, being considered a food rich in all the essential amino acids besides having a high digestibility quality (Bailey et al., 2020). However, animal farming is increasingly impacting the environmental conditions such as greenhouse effects, and the new food trade dynamics, mainly supported by plant-based foods, are an urgent claim. Nonetheless, questions regarding food quality related to the essential amino-acids protein composition, as in the comparison between vegetable and animal-derived proteins, in which unreal claims that vegetable protein sources are inferior to animal proteins for being incomplete in essential amino acids (Hertzler et al., 2020), play a key role in a diet choice (Walker et al., 2019).

Choosing a food depends not only on the food quality but mainly on its characteristics related to sensorial acceptance, such as the parameters that can be measured through the texture profile (NISHINARI et al., 2013), which provides intrinsic sensorial information. Traditionally, the texture is evaluated by mechanical methods, performed through compressing, shearing and/or pulling, applied to most solid food products. The most common equipment used for the texture profile analysis (TPA) test is the texturometer (Peleg, 2019), which generally is a two-bite (double compression) type test that responds to the average value of parameters named as hardness, adhesiveness, cohesiveness, brittleness/fracturability, elasticity/springiness, gumminess, chewiness (Nishinari et al., 2019; Peleg, 2019). Nonetheless, an important drawback of the mechanical methods is the destructive character, which means that the tested products cannot be used for other applications. To overcome this condition, several studies have focused on modeling the relation between non-destructive techniques, such as spectroscopy and imaging analysis, and TPA (Ozdogan et al., 2021; Srisawas et al., 2007) to offer an alternative technology for the food industry.

Spectroscopy techniques such as near-infrared (NIR) and mid-infrared (MIR) coupled with chemometrics have been frequently used to predict chemical compositions in complex food matrices mainly due to simpler, faster, and non-destructive characteristics (Assis et al., 2019;

* Corresponding author.
E-mail addresses: paulohmarco@utfpr.edu.br, paulohmarco@gmail.com (P.H. Março).

https://doi.org/10.1016/j.foodcont.2022.109290
Received 9 April 2022; Received in revised form 23 June 2022; Accepted 29 July 2022
Available online 10 August 2022

Table 1
Description of commercial protein samples from animal and vegetable sources.

Sample Code	Flavoring	Specification
Animal-derived proteins		
1	Tropical fruits: Pineapple. banana and orange	Isolated
2	Flavorless	Isolated
3	Cappuccino	Concentrate blend
4	Malted chocolate with chocolate crisps	Concentrate blend
5	Red fruits	Isolated
6	Papaya. banana and apple	Concentrate and hydrolyzed blend
7	Chocolate	Concentrate blend
8	Chocolate	Concentrate
9	Milk cream	Concentrate
10	Brigadiero	Isolated
11	Chocolate	Isolated/Hydrolyzed
12	Cappuccino	Concentrate
13	Vanilla ice cream	Isolated
14	Chocolate	Isolated
15	Coffee	Isolated
16	Caramel	Isolated
17	Chocolate	Concentrate
18	Moccha	Concentrate
19	Banana	Concentrate
20	Cappuccino	Isolated and concentrate
21	Malted chocolate	Concentrate blend
22	Belgian chocolate	Isolated blend
23	Vanilla	Concentrate
24	Chocolate	Concentrate
25	Chocolate	Isolated and Hydrolyzed
26	Vanilla	Concentrate
Vegetable-derived proteins		
27	Muffin with strawberry and banana	Blend (Pea isolated, rice concentrated, pumpkin protein and chia)
28	Cocoa	Brown rice isolated and pea protein
29	Chocolate with hazelnut	Rice and pea
30	Chocolate	Organic brown rice protein
31	Vanilla	Rice and pea
32	Cocoa	Concentrate yellow pea protein
33	Chocolate	Soy isolated
34	Flavorless	Pea protein
35	Strawberry	Isolated soy protein. pea protein. brown rice protein
36	Flavorless	Roasted pumpkin seed
37	Vanilla	Pea protein isolated and rice protein concentrate
38	Flavorless	Brown rice concentrate protein
39	Chocolate	Vegan protein supplement (Pea isolated protein and organic almond protein)
40	Flavorless	Only vegan protein (Pea isolated protein and organic almond protein)
41	Vanilla	Vegan protein supplement (Pea isolated protein and organic almond protein)
42	Banana with cinnamon	Vegan protein supplement (Pea isolated protein and organic almond protein)
43	Flavorless	Pea protein
44	Flavorless	Soy isolated protein. wheat protein and pea protein
45	Chocolate and banana	Hemp protein
46	Cocoa	Organic almond and pea
47	Banana with cinnamon	Organic almond and pea
48	Chocolate	Hemp protein

Lin et al., 2019; Pereira et al., 2020). The NIR still stands out about other techniques and has been promising in the authentication and detection of adulterations in food, reaching advances in its instrumentation, including portable devices, non-invasive character, and the need for little or no sample preparation (Ma, Wang, Chen, Cheng, & Lai, 2017; Pereira et al., 2020). The inclusion of chemometrics in food sciences and technology has increased in recent years, largely thanks to the feasibility of extracting and interpreting information (Callao & Ruisánchez, 2018). The ComDim (Common Dimension) is one of those unsupervised multiblock tools that can relate and reveal the importance of the data block studied (Cariou et al., 2018). A detailed description of the ComDim tool can be found elsewhere (Cariou et al., 2018; El Ghaziri et al., 2016). Briefly, this multiblock tool allows extracting information from a set of samples evaluated by different techniques. One detached advantage is the information regarding the salience of each technique (block), indicating its importance and variability in each dimension. In other words, when saliences are similar, it is possible to correlate among techniques (Mishra et al., 2020; Rocha Baqueta et al., 2021).

Previous studies have evaluated the nutritional quality of commercial protein supplements (Corgneau et al., 2019; Sánchez-Oliver et al., 2018) and whey protein powder has already been evaluated for digestibility and composition in essential amino acids and adulterations in these products have already been investigated (Almeida et al., 2015; Zaukuu et al., 2020). However, the use of multiblock analysis has not been reported in this context to check the relation between the techniques to find out which is the most loaded characteristic related to the texture profile linked to a specific spectral region. Furthermore, to the best of our knowledge, this is the first study in which the ComDim is being used for the discrimination of commercial protein powder from different sources. Therefore, it must be detached that the advantage of using such an approach is the variance weighed to all the techniques involved. In this sense, the objective of this study is to relate the texture profile to short-NIR spectral vibrations through the ComDim multiblock approach to find out which texture profile parameters can be assigned to the spectral vibrations for each protein source.

2. Material and methods

2.1. Samples

Forty-eight different commercial protein supplements were purchased on the e-commerce, twenty-six from animal and twenty-two from vegetable sources. The samples were composed of different brands, flavors, and or lots. Table 1 presents the sample description with the sample code, flavoring, and type of proteins from animal and vegetable sources. The codes found in Table 1 are used to identify them in all the graphs and further discussions. The samples were weighed (7.5 g) and accommodated in transparent plastic packages.

2.2. Acquisition of the near-infrared spectra (NIR)

The NIR spectra were obtained using a JDSU (VIAVI) MicroNIR 1700® equipment for measurements in the region from 900 to 1700 nm. The reflectance reference was measured using a NIR reflectance standard (SpectralonTM, 99% diffuse reflection coefficient) packed in plastic packages equivalent to the ones used for the sample measurements, while the dark reference (the simulation of non-reflection) was obtained with the lamp turned off. The measurements were performed with the equipment temperature of 45 ± 2 °C, as recommended by the manufacturer. The spectral measurements were performed using 50 scans (i.e, each spectrum is an average of 50 spectra), with samples being measured inside the packages, being all measurements done in triplicate, generating a total of 144 spectra.

2.3. Texture profile analysis (TPA)

For the experiment, a total of 7.5 g of each protein sample were added to 2.5 g of wheat flour together with 10 mL of distilled water in a standard recipient (50 mL plastic cup) with a diameter of 50 mm. The addition of wheat was a necessary procedure to allow for the production of a dough that could be measured using the texturometer. The mixtures were homogenized using a spoon for 3–5 min and then immediately analyzed. The samples were submitted to a double compression by a texturometer model TA-XT Express (Stable Micro Systems) through a cylindrical probe P/0.5 (diameter of 12.7 mm) and a 10 kg load cell. The

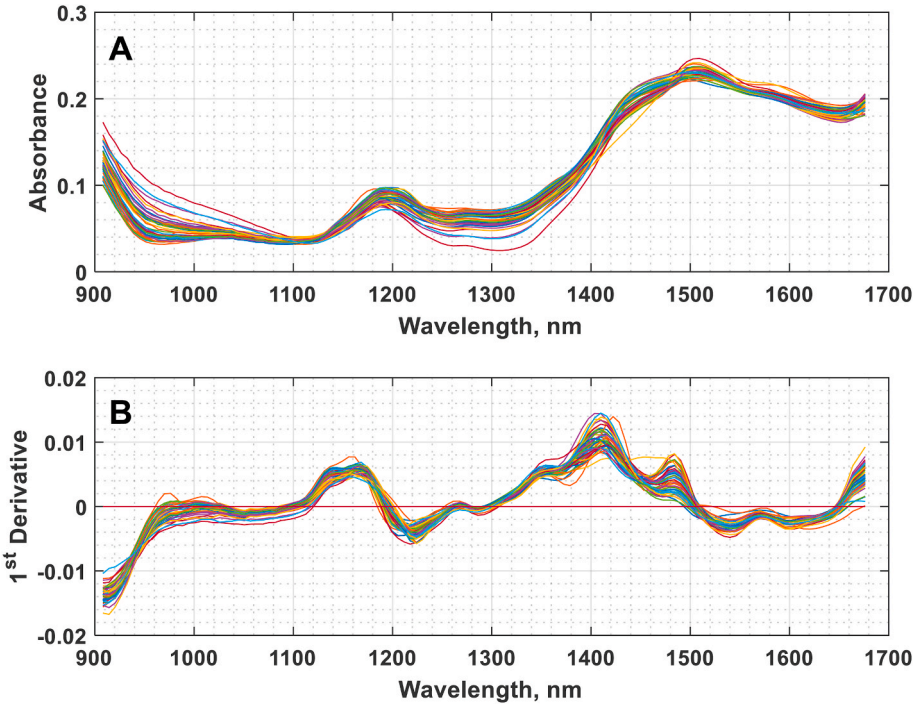

Fig. 1. – NIR spectra from all proteins (**A**) after multiplicative scatter correction and (**B**) after smoothing and the first derivative using 5-point windows and second-order polynomial.

results were processed in Exponent Lite Express software. All tests were carried out at 25 °C and the samples were compressed twice to 50% of their size. The following settings were applied for the analysis: pre-test speed of 1 mm/s, test speed of 1.7 mm/s, the time interval between the two compression cycles was of 5 s, and the trigger force equal to 0.049 N. Ten repetitions were measured per sample. The parameters evaluated were hardness (N), gumminess (N), chewiness (N.mm), resilience, cohesion, springiness, and adhesiveness (N.s) (Mei et al., 2018). The chewiness is generally applicable for solid samples, but not for semi-solids like dough, as such gumminess, considering that gumminess is also related to swallowing. However, although these parameters are related to swallowing, they represent mechanical parameters derived from hardness and, therefore, were considered to evaluate the samples to verify the existing relationships.

2.4. Chemometric analysis

2.4.1. Software

The data obtained were evaluated by using MATLAB version R2021a. The ComDim analysis was performed using a homemade code in which more details can be found in Galvan et al. (2020).

2.4.2. Data pre-processing

The NIR spectra were organized in the form of a matrix, in which each row corresponded to a sample and each column was attributed to a variable (absorbance at different wavelengths and the TPA parameters). Multiplicative scatters correction (MSC) was applied to correct multiplicative and additive dispersion effects, arising from differences between the samples related to the granule size, morphology, and particle orientation (Geladi et al., 1985). The algorithm is based on linear regression of spectral variables versus the average spectrum. In addition, the Savitzky-Golay algorithm (second-degree polynomial with a seven points window) was used to smooth and perform the first derivate on the spectra (Savitzky & Golay, 1964).

2.4.3. Principal component analysis (PCA)

The average spectra of the triplicates were used for the measurements. After preprocessing to correct multiplicative scatter effects, the NIR spectra were mean-centered and the TPA data were autoscaled before the Principal Component Analysis (PCA) to check if there was any difference between proteins according to their sources. PCA is generally used to evaluate patterns inside the data. The algorithm allows for the decomposition of an **X** matrix into two smaller matrices of scores and loadings, where the scores will provide information about the projection of the samples on the new axes, thus allowing to evaluate similarities and differences between the samples, while the loadings will indicate which variables influence the observed projection (Becker--Algeri et al., 2020).

2.4.4. ComDim

The Common Dimensions (ComDim) analysis, derived from the Common Components and Specific Weights Analysis (CCSWA) is an unsupervised multiblock analysis method that aimed initially at solving problems related to sensory analysis (Qannari et al., 1995). It has been used to combine different analysis techniques applied to the same group of samples to compare them (M. Loudiyi, D.N. Rutledge, 2018). For most multivariate analysis methods, a variance-covariance matrix is calculated for the variables. ComDim describes tables that have the same number of rows, but not necessarily the same number of columns, i.e., it evaluates different variables (techniques) for the same set of samples. To do so, the weighted sum of the variance-covariance ($\mathbf{W_i}$) matrices is calculated iteratively. In the first iteration, a weighting, or salience (λ_i) is assumed to be equal to 1 for all the tables (blocks), and the first main component normalized as a Common Dimension (CD) is extracted from the resulting matrix (WG). Then, a new weight estimate is calculated using the initial CD and λ_i values for the new WG calculation until the adjustment's convergence. Therefore, the objective of this tool is to obtain a common space between all the data tables studied, attributing the contribution ("salience") of each block.

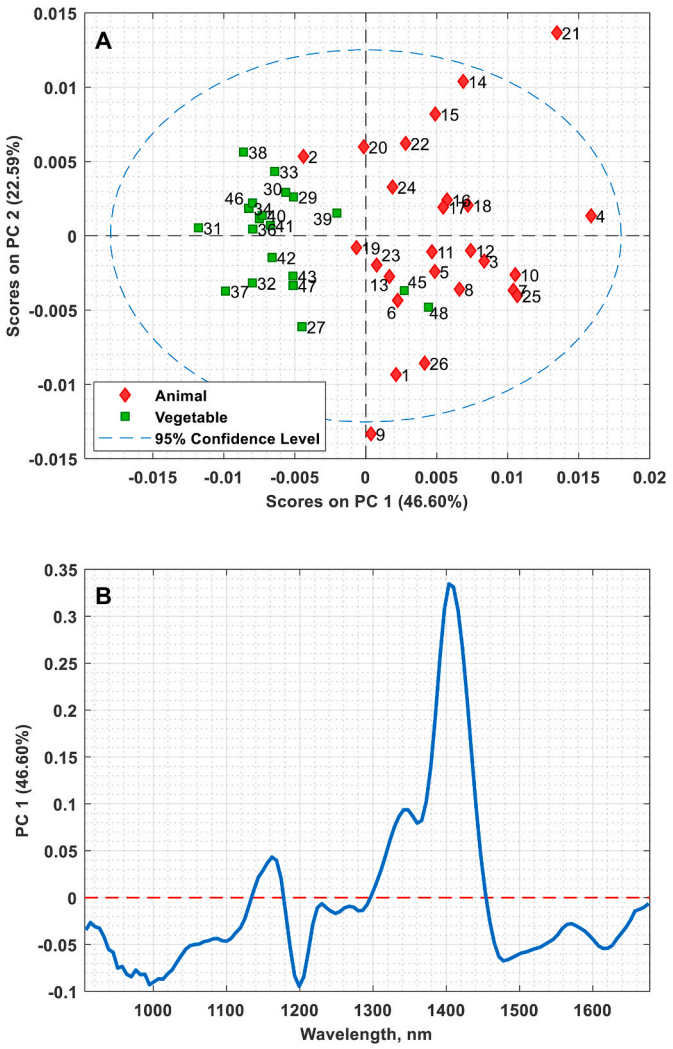

Fig. 2. – Principal Components Analysis plots for the NIR spectral data: (**A**) scores for PC1 (46.60%) vs PC2 (22.59%) and (**B**) loadings for the PC1 (46.60%).

3. Results and discussion

3.1. Near-infrared (NIR) spectroscopy

Fig. 1- A presents the NIR spectra after multiplicative scattering correction, and B the spectra after using the Savitzky-Golay algorithm for smoothing and the first derivative. The Principal Component Analysis (PCA) was applied to the NIR data to explore the similarities between the protein spectra according to the protein source, and the result is shown in Fig. 2 (A) for scores and (B) to the respective loadings. Through the distribution of the scores shown in Fig. 2 (A), it can be noticed that the majority of the proteins are differentiated due to the source (animal or vegetable), being most of the animal-derived protein displaced in positive PC1 values and the vegetable ones at negative PC1 values. Sample 9, which is a milk cream concentrate whey protein sample is outside the 95% confidence level (by assuming that residuals follow a normal distribution). Samples 2 (flavorless whey protein isolated) and 19 (concentrated whey protein - flavor banana) are projected as similar to the vegetable ones, and sample 20 (concentrated and isolated whey protein - flavor cappuccino) is slightly shifted to the negative values of PC1, i.e., similar to the vegetable protein source, even though it is close to zero in PC1. Also, samples 45 (hemp protein flavor chocolate and banana) and 48 (hemp protein flavor chocolate) are distant from the bulk of vegetable samples, being projected as similar to the animal proteins. In these cases, the label suggests that it presents all essential amino acids, such as those of animal origin. Therefore, the distribution of these samples is somehow intriguing and must be better explored by most informative techniques to check for its composition.

Fig. 2 - B presents the loadings of the spectral regions attributed to the separation achieved in Fig. 2 – A. The most intense vibration for positive values on PC1 is located around 1400–1415 nm, which is a region with vibrations characteristic for aliphatic hydrocarbons, such as the C–H (2ν CH_2 & δCH_2) combination, when C–H is associated with linear aliphatic $R(CH_2)_NR$ or associated with branched aliphatic RC $(CH_3)_3$ or $RCH(CH_3)_2$ (Workman Jr. & Weyer, 2012). There is also a signal around 1340–1360 nm, which is usually assigned to C–H from methyls (CH_3) structures, besides the signal in 1160 nm, assigned to the carbonyl (C═O) vibration to aliphatic hydrocarbons. Those achievements are related to animal proteins. On the other hand, the vegetable proteins are characterized by vibrations around 990–1000 nm, added by a signal in 1100 nm, which is a region of O–H vibration that could be from phenols, primary alcohols ($–CH_2–OH$), or even water. Also, there is an important vibration in 1200 nm, which is assigned to O–H vibrations. There are also vibrations around 1520–1530 nm, generally assigned to N–H vibrations, added by a vibration in 1620 nm, assigned to C–H vibrations from alkenes ($=CH_2$) (Workman Jr. & Weyer, 2012). Such above-mentioned regions are responsible for the difference observed between the two protein sources and, according to Ingle et al. (2016), this type of absorption increases according to the protein content present in the sample (Ingle et al., 2016).

3.2. Texture profile analysis (TPA)

The average of 10 measurements to each parameter of the TPA to each sample for the texture profile analysis for the animal and vegetable proteins are presented in Table 2. PCA was applied to check for similarities and the result is shown in Fig. 3 for PC1 (52.64%) vs PC2 (29.48%) as a biplot, i.e, regarding scores and loadings simultaneously.

It is worth noting that the TPA parameters were chosen envisioning the use of the vegetal proteins in diverse used by the food industry such as dough-based foodstuff (Joyner (Melito), 2018). In this sense, parameters like chewiness, gumminess, and springiness may shed some light on the dough's behavior during processing.

PC1 allowed for the separation of the samples according to the protein source, being the vegetable ones projected in positive values of PC1 while animal-derived ones were located in negative values of PC1. The exceptions are samples 45 (hemp protein flavored as chocolate and banana) and 48 (hemp protein flavored as chocolate), which are from vegetable sources and are located as similar to the animal ones, and sample 22 (isolated whey protein flavored as chocolate), projected as being similar to the vegetable ones.

According to the loadings, the animal-derived proteins are associated with adhesiveness and springiness, while the parameters of cohesiveness, chewiness, gumminess, hardness, and resilience were assigned to the similarity observed between proteins from vegetable sources.

Previous studies have shown that vegetable proteins (textured pea

Table 2
Results for Texture Profile Analysis (TPA) of commercial animal and vegetable proteins.

Animal-derived proteins							
Sample	Hardness (N)	Adhesiveness (N.s)	Springiness	Chewiness (N.mm)	Gumminess (N)	Cohesion;	Resilience
1	0.33 ± 0.04	−0.39 ± 0.10	0.97 ± 0.02	20.65 ± 2.93	21.24 ± 2.84	0.63 ± 0.04	0.08 ± 0.01
2	0.18 ± 0.05	−0.17 ± 0.01	0.97 ± 0.01	12.34 ± 4.64	12.75 ± 4.71	0.69 ± 0.05	0.06 ± 0.01
3	0.15 ± 0.03	−0.18 ± 0.01	0.96 ± 0.01	9.42 ± 2.46	9.76 ± 2.48	0.63 ± 0.04	0.04 ± 0.01
4	0.29 ± 0.07	−0.39 ± 0.05	0.96 ± 0.01	17.36 ± 5.02	17.98 ± 5.03	0.60 ± 0.03	0.07 ± 0.01
5	0.30 ± 0.05	−0.59 ± 0.12	0.97 ± 0.01	18.88 ± 3.67	19.39 ± 3.69	0.64 ± 0.09	0.05 ± 0.01
6	0.33 ± 0.06	−0.54 ± 0.10	0.95 ± 0.02	17.48 ± 3.93	18.36 ± 3.95	0.55 ± 0.06	0.06 ± 0.01
7	0.31 ± 0.09	−0.41 ± 0.05	0.97 ± 0.01	19.73 ± 5.80	20.23 ± 5.93	0.64 ± 0.03	0.04 ± 0.01
8	0.36 ± 0.02	0.62 ± 0.04	0.96 ± 0.00	21.76 ± 1.82	22.62 ± 1.84	0.61 ± 0.03	0.06 ± 0.01
9	0.29 ± 0.07	−0.37 ± 0.03	0.98 ± 0.00	18.47 ± 5.38	18.90 ± 5.49	0.64 ± 0.02	0.04 ± 0.01
10	0.26 ± 0.03	−0.55 ± 0.03	0.96 ± 0.01	15.20 ± 2.12	15.87 ± 2.13	0.61 ± 0.04	0.04 ± 0.01
11	0.29 ± 0.06	−0.41 ± 0.03	0.97 ± 0.00	17.64 ± 4.55	18.21 ± 4.66	0.62 ± 0.02	0.04 ± 0.01
12	0.39 ± 0.31	0.61 ± 0.04	0.96 ± 0.01	17.64 ± 2.36	18.42 ± 2.41	0.62 ± 0.03	0.05 ± 0.01
13	0.47 ± 0.24	−0.41 ± 0.09	0.98 ± 0.01	33.92 ± 18.56	34.66 ± 18.95	0.70 ± 0.05	0.10 ± 0.05
14	0.15 ± 0.06	−0.23 ± 0.04	0.92 ± 0.01	9.60 ± 4.15	10.45 ± 4.45	0.69 ± 0.02	0.05 ± 0.01
15	0.12 ± 0.01	−0.22 ± 0.02	0.92 ± 0.01	7.84 ± 0.86	8.49 ± 0.95	0.68 ± 0.02	0.06 ± 0.01
16	0.15 ± 0.04	−0.36 ± 0.09	0.97 ± 0.01	9.65 ± 2.35	9.97 ± 2.36	0.64 ± 0.01	0.03 ± 0.00
17	0.24 ± 0.14	−0.17 ± 0.02	0.97 ± 0.03	16.21 ± 9.81	16.63 ± 9.71	0.68 ± 0.06	0.06 ± 0.04
18	0.25 ± 0.04	−0.49 ± 0.04	0.96 ± 0.03	15.34 ± 3.40	15.98 ± 3.39	0.62 ± 0.03	0.04 ± 0.01
19	0.27 ± 0.02	−0.56 ± 0.05	0.95 ± 0.01	15.18 ± 1.25	15.91 ± 1.21	0.58 ± 0.03	0.06 ± 0.01
20	0.24 ± 0.02	−0.39 ± 0.06	0.96 ± 0.01	13.34 ± 1.43	13.89 ± 1.46	0.57 ± 0.03	0.06 ± 0.01
21	0.26 ± 0.03	−0.40 ± 0.06	0.96 ± 0.02	14.24 ± 2.05	14.86 ± 1.98	0.57 ± 0.03	0.06 ± 0.01
22	2.27 ± 0.17	−1.12 ± 0.50	0.85 ± 0.08	113.91 ± 16.43	133.38 ± 8.21	0.58 ± 0.06	0.11 ± 0.01
23	0.17 ± 0.07	−0.18 ± 0.03	0.97 ± 0.01	11.83 ± 5.86	12.17 ± 5.88	0.69 ± 0.05	0.05 ± 0.02
24	0.16 ± 0.01	−0.33 ± 0.04	0.95 ± 0.01	9.52 ± 0.44	10.00 ± 0.47	0.64 ± 0.04	0.05 ± 0.01
25	0.27 ± 0.03	−0.37 ± 0.06	0.97 ± 0.01	16.36 ± 3.08	16.80 ± 3.02	0.60 ± 0.03	0.07 ± 0.01
26	0.30 ± 0.09	−0.40 ± 0.05	0.97 ± 0.01	17.74 ± 7.21	18.24 ± 7.21	0.58 ± 0.05	0.06 ± 0.01
Vegetable-derived proteins							
27	0.68 ± 0.10	−1.24 ± 0.18	0.97 ± 0.01	48.16 ± 6.12	49.62 ± 6.16	0.71 ± 0.04	0.07 ± 0.01
28	1.39 ± 0.32	−2.22 ± 0.27	0.55 ± 0.12	38.05 ± 7.55	69.92 ± 5.59	0.51 ± 0.09	0.10 ± 0.01
29	1.24 ± 0.25	−2.21 ± 0.25	0.53 ± 0.06	32.65 ± 5.11	62.11 ± 8.42	0.50 ± 0.05	0.08 ± 0.01
30	0.98 ± 0.14	−2.04 ± 0.20	0.75 ± 0.16	44.35 ± 12.51	59.02 ± 4.43	0.60 ± 0.10	0.08 ± 0.01
31	0.72 ± 0.15	−1.47 ± 0.36	0.91 ± 0.09	44.42 ± 4.82	49.20 ± 5.58	0.68 ± 0.06	0.08 ± 0.01
32	0.83 ± 0.23	−1.74 ± 0.39	0.87 ± 0.12	48.67 ± 5.36	56.56 ± 9.26	0.69 ± 0.07	0.08 ± 0.01
33	3.33 ± 0.54	−1.89 ± 0.53	0.94 ± 0.06	193.31 ± 27.82	207.15 ± 31.18	0.61 ± 0.03	0.11 ± 0.01
34	2.42 ± 0.43	−2.13 ± 0.78	0.93 ± 0.05	151.62 ± 19.32	162.42 ± 21.16	0.66 ± 0.05	0.11 ± 0.01
35	2.15 ± 0.34	−3.26 ± 0.90	0.96 ± 0.04	147.40 ± 14.48	154.40 ± 14.45	0.71 ± 0.06	0.09 ± 0.01
36	0.63 ± 0.11	−1.22 ± 0.28	0.96 ± 0.01	42.40 ± 7.10	44.13 ± 7.23	0.69 ± 0.02	0.07 ± 0.00
37	0.65 ± 0.11	−1.26 ± 0.33	0.94 ± 0.06	42.71 ± 6.28	45.68 ± 6.72	0.69 ± 0.04	0.08 ± 0.01
38	0.81 ± 0.10	−1.89 ± 0.14	0.96 ± 0.01	59.03 ± 6.11	61.27 ± 6.29	0.74 ± 0.02	0.07 ± 0.01
39	0.98 ± 0.04	−1.91 ± 0.10	0.97 ± 0.00	72.45 ± 3.83	74.73 ± 3.79	0.75 ± 0.02	0.08 ± 0.01
40	1.61 ± 0.12	−2.80 ± 0.48	0.98 ± 0.01	117.60 ± 10.29	120.71 ± 9.80	0.74 ± 0.04	0.07 ± 0.01
41	0.92 ± 0.13	−1.99 ± 0.23	0.97 ± 0.00	68.45 ± 9.25	70.56 ± 9.47	0.76 ± 0.02	0.07 ± 0.01
42	0.83 ± 0.05	−1.93 ± 0.12	0.97 ± 0.00	62.19 ± 4.93	64.11 ± 5.12	0.76 ± 0.03	0.07 ± 0.01
43	1.44 ± 0.15	−2.24 ± 0.29	0.97 ± 0.01	108.66 ± 11.53	111.52 ± 11.10	0.76 ± 0.01	0.10 ± 0.01
44	2.91 ± 0.35	−1.22 ± 0.62	0.87 ± 0.08	165.25 ± 23.61	189.56 ± 17.70	0.64 ± 0.05	0.14 ± 0.02
45	0.44 ± 0.07	−0.77 ± 0.23	0.96 ± 0.01	28.83 ± 4.29	29.97 ± 4.68	0.67 ± 0.02	0.08 ± 0.01
46	0.74 ± 0.07	−1.30 ± 0.18	0.95 ± 0.03	50.88 ± 2.86	53.31 ± 3.00	0.71 ± 0.04	0.09 ± 0.01
47	0.77 ± 0.39	−1.27 ± 0.20	0.94 ± 0.05	46.30 ± 5.40	49.33 ± 6.52	0.73 ± 0.05	0.08 ± 0.01
48	0.52 ± 0.30	−0.68 ± 0.17	0.97 ± 0.00	28.10 ± 4.33	28.98 ± 4.49	0.67 ± 0.02	0.07 ± 0.01

protein) tend to be less dense and more porous, and consequently less resistant to compression forces, and can physically return about 90% of their original dimension after being compressed. Therefore, they are also more elastic (Webb et al., 2020). Zhu et al. (2021) observed similar results in textured peanut protein (Zhu et al., 2021). However, according to the authors, protein-protein interactions may suffer interference from starch. The proportion of amylose:amylopectin in vegetables depends on the botanical source and also on the degree of maturation of the plant, considering that higher levels of amylose can confer greater hardness (Nakamura et al., 2021).

3.3. Multi-Block Analysis (ComDim)

Combining the results of the two techniques used by the ComDim analysis allows to improve the interpretability of the results and infer more accurately the consensus relating the different techniques, and, consequently, the similarities between the two sources of protein. For the implementation of ComDim, a matrix was built by merging the NIR and TPA. In this case, the first common dimension (CD1) explained 86.81% of the total data variance. Fig. 4 shows the ComDim results regarding (A) the saliences, (B) the global scores shared in the first

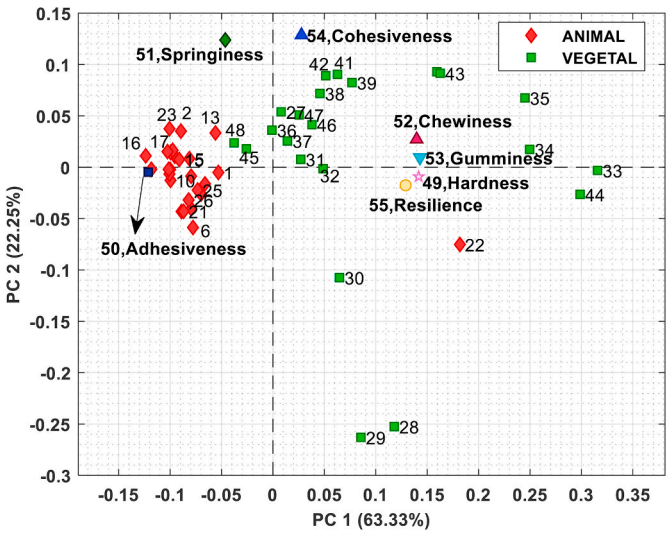

Fig. 3. – Principal Components Analysis biplot for the PC1 (63.33%) vs PC2 (22.25%) of the texturometer data.

common dimension, (C) the NIR loadings for this dimension related with the (D) TPA loadings. The variables with the highest loadings values present greater variance and are responsible for the differentiation of the samples.

In the first common dimension, the global scores (Fig. 4 – B), 1 sample from animal protein (sample 22, isolated whey protein flavored as chocolate) was displayed as similar to the vegetable ones, while samples 45 (hemp protein flavor chocolate and banana) and 48 (hemp protein flavor chocolate) were located as similar to the animal ones. These results agree with the TPA scores, which are the most important scores according to the saliences (Fig. 4 – A). One of the hypotheses for the similarity observed between samples 45 and 48, which are of vegetable origin, with samples of animal origin is due to the compositional character, according to the information on the label, that they have quantities of essential amino acids comparable to samples of proteins of animal origin. Samples 45 and 48 were attributed to proteins extracted from the hemp plant (cannabis derivative), an unusual and not very popular plant, since it is a food whose cultivation is prohibited in most countries, resulting in its restricted use. Regarding sample 22, there is no evident reason for the shifting, which implies that it needs to be explored by more informative techniques to find a reasonable explanation for it.

The correlation of the samples (Fig. 4 – B) to the variables (Fig. 4 – C, regarding NIR spectra, and Fig. 4 – D, regarding TPA) can be evaluated by checking the distribution between them (positive/negative). Therefore, vegetable-derived proteins, which are located with positive values in CD1, are correlated with the NIR region between 900 and 1120 nm, 1180–1220 nm, 1250–1295 nm, and 1460–1700 nm (Fig. 4 – C), also with positive values, as well as hardness, chewiness, gumminess, cohesiveness, and resilience, in Fig. 4 - D. The region around 940 nm is mainly assigned to C–H vibrations for aliphatic hydrocarbons. Nonetheless, the region from 1015 to 1026 nm presents various different N–H vibrations, which is the main protein characteristic. Above 1170 nm, there is an alkene (polyenes) characteristic C–H vibration, followed by vibrations that are characteristic of C–H aliphatic vibration (CH_3), such as 1194, 1195 nm. This is also a region for C–H vibrations of CH_2 from methylenic compounds (1211–1215 nm). Nonetheless, the most important vibrations are located at 1510 and 1630 nm. Signals situated from 1500 to 1520 nm are assigned to several N–H vibrations forms, which can be a result of the amine groups on the protein composition. The signals found between 1600 and 1640 nm can be assigned to C–H from vinylic groups, characteristic of vegetable-derived fats.

Considering the negative values assigned to animal-derived proteins (except sample 22), the correlation bounds the animal-derived proteins with the NIR regions from 1120 to 1180 nm, with a minimal correlation with the region between 1220 and 1240 and mainly the region from 1300 to 1460 nm. Those are primarily correlated with adhesiveness but also with springiness. At 1225 nm, there is a characteristic C–H vibration of secondary or tertiary aliphatic hydrocarbons. Also, at 1360 nm there is a characteristic vibration of methyl C–H from aliphatic hydrocarbons at 1440 nm. From 1441 to 1448, the signals are typical of N–H vibrations, consistent with the protein compositions.

Generally, TPA is used to compare vegetables before and after processing, i.e., fresh and processed. Therefore, we could not find any robust study to compare the characteristics between vegetable and animal-derived proteins. Nonetheless, based on the composition, it is well known that the fats found in animal-derived products are richer in saturated hydrocarbons such as cholesterol, being absent in vegetable sources, while phytosterols either do not exist in animal-based products or have trace amounts (Zarabadipour et al., 2021). It is also important to report that the differentiation was achieved even with impurities, indicating that the protein source is more important in differentiating between proteins than the additives, such as vitamins, colorants, and flavorings.

4. Conclusion

The ComDim multiblock approach allowed for the differentiation of proteins regarding the source (animal or vegetal), besides correlating these samples with the variables from NIR spectroscopy to the texture profile analysis parameters even in the presence of impurities. For vegetable-derived proteins, the NIR regions between 900 and 1120 nm, 1180–1220 nm, 1250–1295 nm, and 1460–1700 nm were related to hardness, chewiness, gumminess, cohesiveness, and resilience. On the other hand, for the animal-derived proteins, the NIR regions from 1120 to 1180 nm, and from 1300 to 1460 nm are correlated mainly with adhesiveness, but also with springiness. Also, ComDim performance was coherently when evaluating each technique (NIR and TPA) individually through PCA, suggesting that ComDim can be used as a tool to correlate techniques to find out relations between samples and variables provided from different techniques.

The results indicated that this approach has the potential to be used both in the differentiation of proteins for restrictive consumers, as for vegans and vegetarians, as well as in highlighting NIR regions to propose quantitative models to predict the characteristics of foods enriched with different proteins.

CRediT authorship contribution statement

Marcela de Souza Zangirolami: Data curation, Formal analysis, Investigation, Methodology, Writing – original draft. **Thaysa Fernandes Moya Moreira:** TPA analysis, Methodology. **Fernanda Vitória Leimann:** Investigation, TPA analysis, Methodology. **Patrícia Valderrama:** Conceptualization, Investigation, Writing – review & editing.

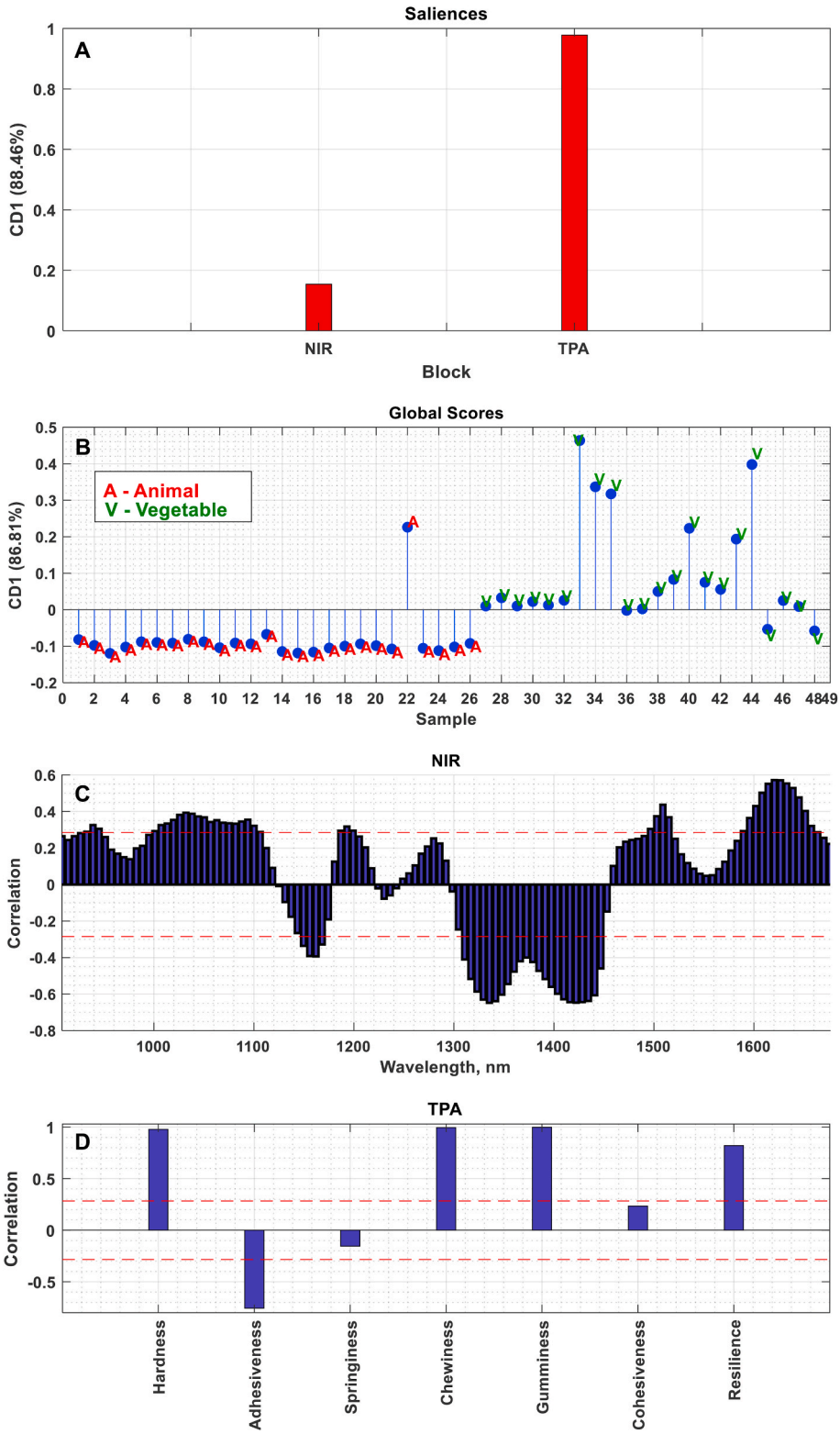

Fig. 4. – Multi-Block Analysis (ComDim): (**A**) Global Scores, (**B**) NIR Loadings, and **(C)** TPA Loadings. The red-dashed-lines ((----)) refers to 2 times standard deviation interval.

Paulo Henrique Março: Conceptualization, Supervision, Funding acquisition, Formal analysis, Investigation, Data curation, Writing – review & editing.

Declaration of competing interest

The authors declare that they have no known competing financial interests or personal relationships that could have appeared to influence the work reported in this paper.

Data availability

Data will be made available on request.

Acknowledgments

This work was supported by the Coordenação de Aperfeiçoamento de Pessoal de Nível Superior (CAPES) Brazil [grant number 001]. Patrícia Valderrama is grateful for Conselho Nacional de Pesquisa (CNPq - process 306606/2020–8).

References

Almeida, C. C., Monteiro, M. L. G., Costa-Lima, B. R. C. da, Alvares, T. S., & Conte-Junior, C. A. (2015). In vitro digestibility of commercial whey protein supplements. *LWT - Food Science and Technology, 61*(1), 7–11. https://doi.org/10.1016/j.lwt.2014.11.038

Assis, C., Pereira, H. V., Amador, V. S., Augusti, R., de Oliveira, L. S., & Sena, M. M. (2019). Combining mid infrared spectroscopy and paper spray mass spectrometry in a data fusion model to predict the composition of coffee blends. *Food Chemistry, 281*, 71–77. https://doi.org/10.1016/j.foodchem.2018.12.044

Bailey, H. M., Mathai, J. K., Berg, E. P., & Stein, H. H. (2020). Most meat products have digestible indispensable amino acid scores that are greater than 100, but processing may increase or reduce protein quality. *British Journal of Nutrition*. https://doi.org/10.1017/S0007114520000641. February.

Becker-Algeri, T. A., Souza, C., Bortoli, K., Castagnaro, D., Scaglioni, P. T., Drunkler, D. A., Dors, G., Valderrama, P., & Badiale-Furlong, E. (2020). Seasonal variation of milk quality: Physicochemical, microbiological, and toxicological. *Journal of Food Safety, 1*(October 2018), 1–12. https://doi.org/10.1111/jfs.12796

Callao, M. P., & Ruisánchez, I. (2018). An overview of multivariate qualitative methods for food fraud detection. *Food Control, 86*, 283–293. https://doi.org/10.1016/j.foodcont.2017.11.034

Cariou, V., Qannari, E. M., Rutledge, D. N., & Vigneau, E. (2018). ComDim: From multiblock data analysis to path modeling. *Food Quality and Preference, 67*, 27–34. https://doi.org/10.1016/j.foodqual.2017.02.012

Corgneau, M., Gaiani, C., Petit, J., Nikolova, Y., Banon, S., Ritié-Pertusa, L., Le, D. T. L., & Scher, J. (2019). Nutritional quality evaluation of commercial protein supplements. *International Journal of Food Science and Technology, 54*(8), 2586–2594. https://doi.org/10.1111/ijfs.14170

El Ghaziri, A., Cariou, V., Rutledge, D. N., & Qannari, E. M. (2016). Analysis of multiblock datasets using ComDim: Overview and extension to the analysis of (K + 1) datasets. *Journal of Chemometrics, 30*(8), 420–429. https://doi.org/10.1002/cem.2810

Galvan, D., Bona, E., Borsato, D., Danieli, E., & Henrique Montazzolli Killner, M. (2020). Calibration transfer of partial least squares regression models between desktop nuclear magnetic resonance spectrometers. *Analytical Chemistry, 92*(19), 12809–12816. https://doi.org/10.1021/acs.analchem.0c00902

Geladi, P., MacDougall, D., & Martens, H. (1985). Linearization and scatter-correction for near-infrared reflectance spectra of meat. *Applied Spectroscopy, 39*(3), 491–500. https://doi.org/10.1366/0003702854248656

Hertzler, S. R., Lieblein-Boff, J. C., Weiler, M., & Allgeier, C. (2020). Plant proteins: Assessing their nutritional quality and effects on health and physical function. *Nutrients, 12*(12), 3704. https://doi.org/10.3390/nu12123704

Ingle, P. D., Christian, R., Purohit, P., Zarraga, V., Handley, E., Freel, K., & Abdo, S. (2016). Determination of protein content by NIR spectroscopy in protein powder mix products. *Journal of AOAC International, 99*(2), 360–363. https://doi.org/10.5740/jaoacint.15-0115

Joyner (Melito), H. S. (2018). Explaining food texture through rheology. *Current Opinion in Food Science, 21*, 7–14. https://doi.org/10.1016/j.cofs.2018.04.003

Lin, L., He, Y., Xiao, Z., Zhao, K., Dong, T., & Nie, P. (2019). Rapid-detection sensor for rice grain moisture based on NIR spectroscopy. *Applied Sciences, 9*(8). https://doi.org/10.3390/app9081654

Loudiyi, M., Rutledge, D. N., & A. A.-K. (2018). ComDim for explorative multi-block data analysis of Cantal-type cheeses: Effects of salts, gentle heating and ripening. *Food Chemistry, 264*, 401–410. https://doi.org/10.1016/j.foodchem.2018.05.039

Mei, M. S., Goh, A. T., Stieger, M., & Forde, C. G. (2018). Correlation of instrumental texture properties from textural profile analysis (TPA) with eating behaviours and macronutrient composition for a wide range of solid foods. *Food & Function, 9*(10), 5301–5312. https://doi.org/10.1039/c8fo00791h

Mishra, P., Roger, J. M., Rutledge, D. N., Biancolillo, A., Marini, F., Nordon, A., & Jouan-Rimbaud-Bouveresse, D. (2020). MBA-GUI: A chemometric graphical user interface for multi-block data visualisation, regression, classification, variable selection and automated pre-processing. *Chemometrics and Intelligent Laboratory Systems, 205*, Article 104139. https://doi.org/10.1016/J.CHEMOLAB.2020.104139

Nakamura, S., Katsura, J., Maruyama, Y., & Ohtsubo, K. (2021). Evaluation of hardness and retrogradation of cooked rice based on its pasting properties using a novel RVA testing. *Foods, 10*(5), 987. https://doi.org/10.3390/foods10050987

Nishinari, K., Fang, Y., & Rosenthal, A. (2019). Human oral processing and texture profile analysis parameters: Bridging the gap between the sensory evaluation and the instrumental measurements. *Journal of Texture Studies, 50*(5), 369–380. https://doi.org/10.1111/jtxs.12404

Nishinari, K., Kohyama, K., Kumagai, H., Funami, T., & Bourne, M. C. (2013). Parameters of texture profile Analysis. *Food Science and Technology Research, 19*(3), 519–521. https://doi.org/10.3136/fstr.19.519

Ozdogan, G., Lin, X., & Sun, D.-W. (2021). Rapid and noninvasive sensory analyses of food products by hyperspectral imaging: Recent application developments. *TRENDS IN FOOD SCIENCE \& TECHNOLOGY, 111*, 151–165. https://doi.org/10.1016/j.tifs.2021.02.044

Peleg, M. (2019). The instrumental texture profile analysis revisited. *Journal of Texture Studies, 50*(5), 362–368. https://doi.org/10.1111/jtxs.12392

Pereira, E. V., dos, S., Fernandes, D. D. de S., de Araújo, M. C. U., Diniz, P. H. G. D., & Maciel, M. I. S. (2020). Simultaneous determination of goat milk adulteration with cow milk and their fat and protein contents using NIR spectroscopy and PLS algorithms. *Lwt, 127*(April), Article 109427. https://doi.org/10.1016/j.lwt.2020.109427

Qannari, E. M., Wakeling, I., & MacFie, H. J. H. (1995). A hierarchy of models for analysing sensory data. *Food Quality and Preference, 6*(4), 309–314. https://doi.org/10.1016/0950-3293(95)00033-X

Rocha Baqueta, M., Coqueiro, A., Henrique Março, P., Mandrone, M., Poli, F., & Valderrama, P. (2021). Integrated 1H NMR fingerprint with NIR spectroscopy, sensory properties, and quality parameters in a multi-block data analysis using ComDim to evaluate coffee blends. *Food Chemistry, 355*, Article 129618. https://doi.org/10.1016/J.FOODCHEM.2021.129618

Sánchez-Oliver, A. J., Contreras-Calderón, J., Puya-Braza, J. M., & Guerra-Hernández, E. (2018). Quality analysis of commercial protein powder supplements and relation to characteristics declared by manufacturer. *Lwt, 97*(February), 100–108. https://doi.org/10.1016/j.lwt.2018.06.047

Savitzky, A., & Golay, M. J. E. (1964). Smoothing and differentiation of data by simplified least squares procedures. *Analytical Chemistry, 36*(8), 1627–1639. https://doi.org/10.1021/ac60214a047

Srisawas, W., Jindal, V. K., & Thanapase, W. (2007). Relationship between sensory textural attributes and near infrared spectra of cooked rice. *JOURNAL OF NEAR INFRARED SPECTROSCOPY, 15*(5), 333–340. https://doi.org/10.1255/jnirs.746

Walker, C., Gibney, E. R., Mathers, J. C., & Hellweg, S. (2019). Comparing environmental and personal health impacts of individual food choices. *Science of the Total Environment, 685*, 609–620. https://doi.org/10.1016/j.scitotenv.2019.05.404

Webb, D., Plattner, B. J., Donald, E., Funk, D., Plattner, B. S., & Alavi, S. (2020). Role of chickpea flour in texturization of extruded pea protein. *Journal of Food Science, 85*(12), 4180–4187. https://doi.org/10.1111/1750-3841.15531

Workman, J., Jr., & Weyer, L. (2012). Practical guide and spectral Atlas for interpretive near-infrared spectroscopy. In *Practical guide and spectral Atlas for interpretive near-infrared spectroscopy, Sercond edition spectroscopy* (2nd ed., pp. i–xvi). CRC Press. https://doi.org/10.1201/b11894-1.

Zarabadipour, F., Piravi-Vanak, Z., & Aminifar, M. (2021). Evaluation of sterol composition in different formulations of cocoa milk as milk fat purity indicator. *Food Science and Technology, 41*(2), 519–523. https://doi.org/10.1590/fst.06520

Zaukuu, J. L. Z., Aouadi, B., Lukács, M., Bodor, Z., Vitális, F., Gillay, B., Gillay, Z., Friedrich, L., & Kovacs, Z. (2020). Detecting low concentrations of nitrogen-based Adulterants in whey protein powder using benchtop and handheld NIR spectrometers and the feasibility of scanning through plastic bag. *Molecules (Basel, Switzerland), 25*(11), 1–15. https://doi.org/10.3390/molecules25112522

Zhu, D., Fang, C., Qian, Z., Guo, B., & Huo, Z. (2021). Differences in starch structure, physicochemical properties and texture characteristics in superior and inferior grains of rice varieties with different amylose contents. *Food Hydrocolloids, 110*(July 2020), Article 106170. https://doi.org/10.1016/j.foodhyd.2020.106170

Further reading

Hever, J. (2016). Plant-based diets: A physician's guide summary of health benefits. *The Permanente Journal/Perm J 2016 Summer Perm J 2016 Summer, 2020*(33), 15–82. https://doi.org/10.7812/TPP/15-082

Mathai, J. K., Liu, Y., & Stein, H. H. (2017). Values for digestible indispensable amino acid scores (DIAAS) for some dairy and plant proteins may better describe protein quality than values calculated using the concept for protein digestibility-corrected amino acid scores (PDCAAS). *British Journal of Nutrition, 117*(4), 490–499. https://doi.org/10.1017/S0007114517000125